Diffractive Photoproduction of J/ψ Mesons with Large Momentum Transfer at HERA

H1 Collaboration

Abstract

The diffractive photoproduction of J/ψ mesons is measured with the H1 detector at the ep collider HERA using an integrated luminosity of 78 pb^{-1}. The differential cross section $\mathrm{d}\sigma(\gamma p \to J/\psi Y)/\mathrm{d}t$ is studied in the range $2 < |t| < 30$ GeV^2, where t is the square of the four-momentum transferred at the proton vertex. The cross section is also presented as a function of the photon-proton centre-of-mass energy $W_{\gamma p}$ in three t-intervals, spanning the range $50 < W_{\gamma p} < 200$ GeV. A fast rise of the cross section with $W_{\gamma p}$ is observed for each t range and a slope for the effective linear Pomeron trajectory of $\alpha'_{I\!P} = -0.0134 \pm 0.0074(stat.) \pm 0.0065(syst.)$ GeV^{-2} is obtained. Perturbative QCD models based on BFKL and DGLAP evolution are able to provide a general description of the data. The data are found to be compatible with s-channel helicity conservation.

Prepared for DIS 2003, St.Petersburg

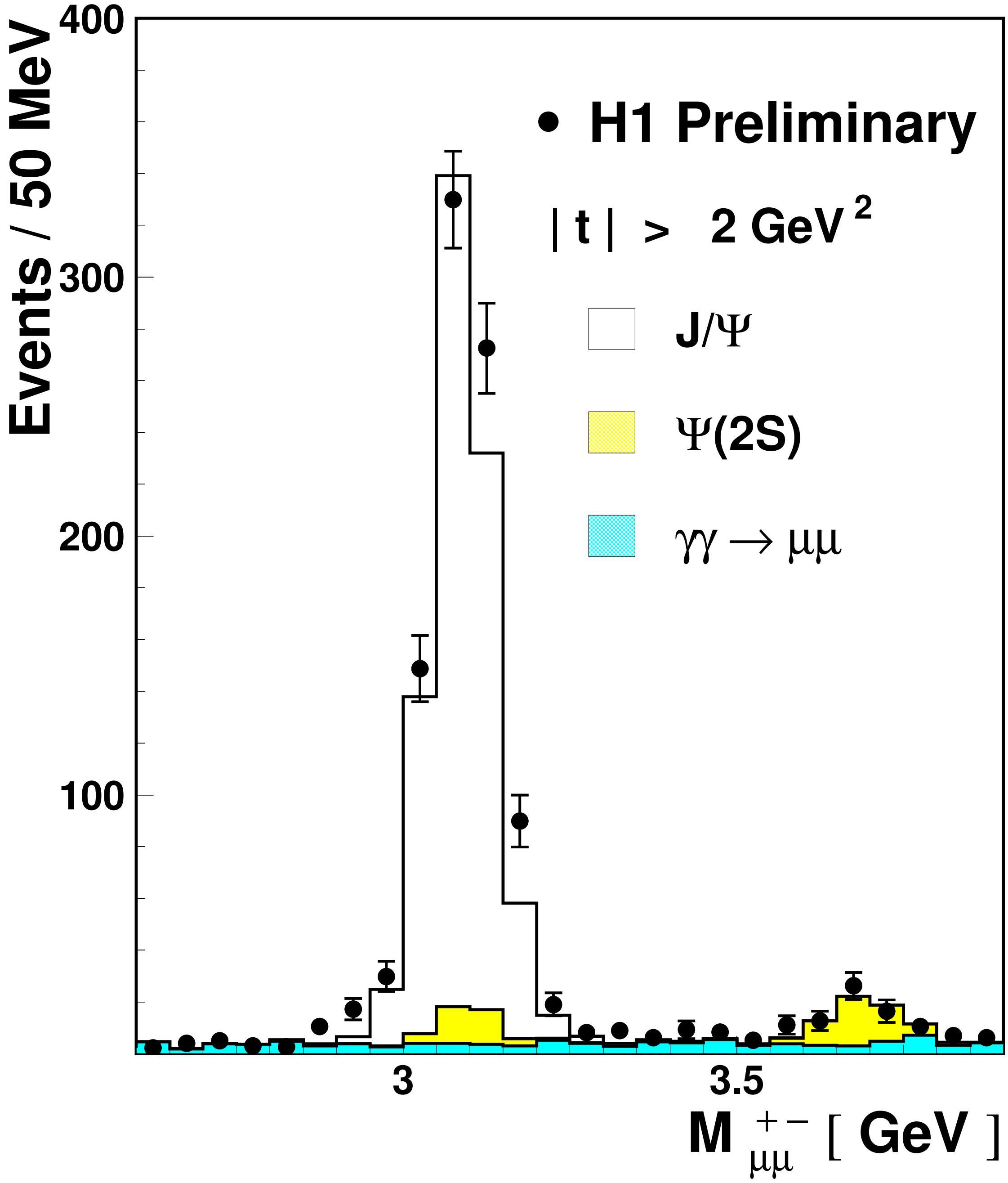

Figure 1: The $\mu^+\mu^-$ invariant mass distribution after final selection cuts in the kinematic region $|t| > 2\ \mathrm{GeV}^2$. The histogram shows the sum of the Monte Carlo simulations of J/ψ production using HITVM (open histogram), the contribution from lepton pair production as simulated by the LPAIR program (dark shaded histogram) and the contribution from diffractive $\psi(2S)$ events as simulated with the DIFFVM program (light shaded histogram).

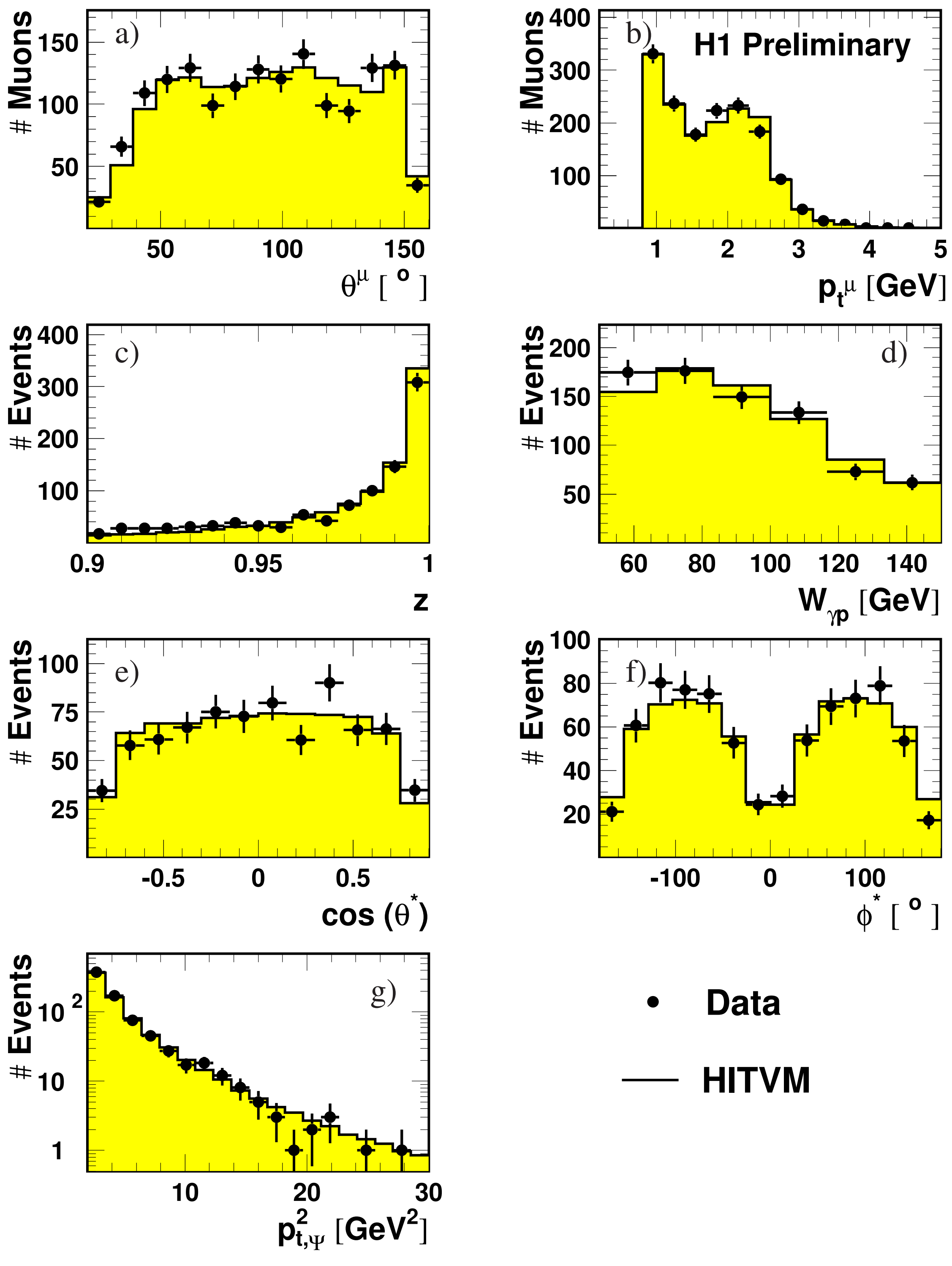

Figure 2: Kinematic distributions of the J/ψ meson and its decay lepton tracks for events in the mass range $2.9 < M_{\mu^+\mu^-} < 3.3$ GeV. a) The polar angle θ^μ and b) the transverse momentum p_t^μ of the decay lepton tracks. c) The inelasticity z and d) the photon-proton centre of mass energy $W_{\gamma p}$ of the J/ψ meson. e) The distribution of the cosine of the polar angle and f) the azimuthal distribution of the positively charged decay muon in the helicity frame. g) The distribution of the squared transverse momentum of the J/ψ. The data are shown by the points and the HITVM Monte Carlo simulation by the shaded histogram.

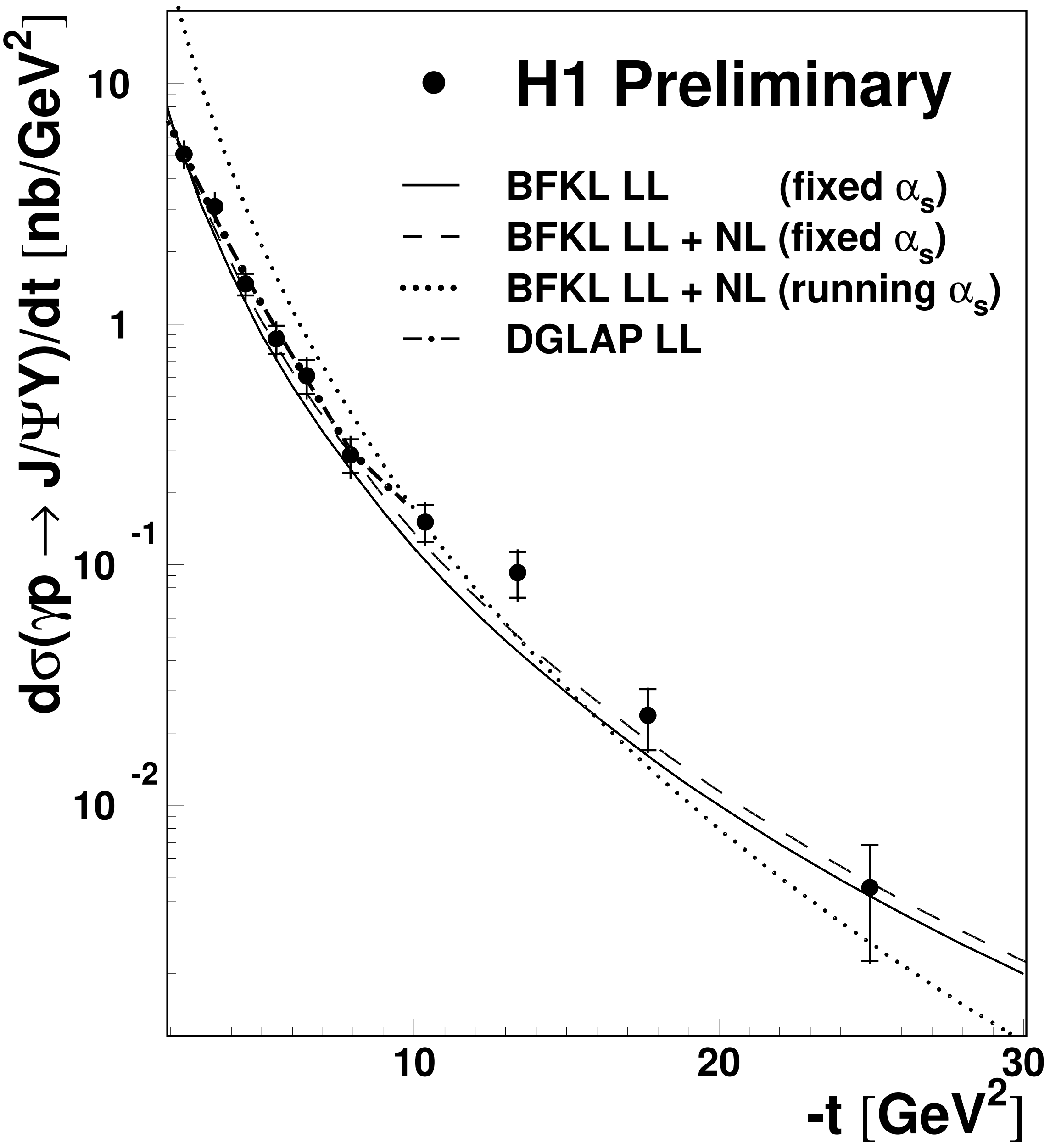

Figure 3: The photon-proton differential cross section $\mathrm{d}\sigma/\mathrm{d}t$ for J/ψ production in the kinematic range $50 < W_{\gamma p} < 150$ GeV, $|t| > 2.0$ GeV^2 and $z > 0.95$. The inner error bars correspond to the statistical error, the outer error bars are the statistical and systematic errors added in quadrature. The solid line shows the prediction from the BFKL calculation in the leading log approximation for fixed $\alpha_S = 0.18$ [?]. The dashed (dotted) curve corresponds to the BFKL calculation including non-leading corrections and using a fixed (running) α_S [?]. Also shown (dashed-dotted curve in the range $-t < M^2_{J/\psi}$) is the result of a calculation based on the DGLAP equation in the leading log approximation [?].

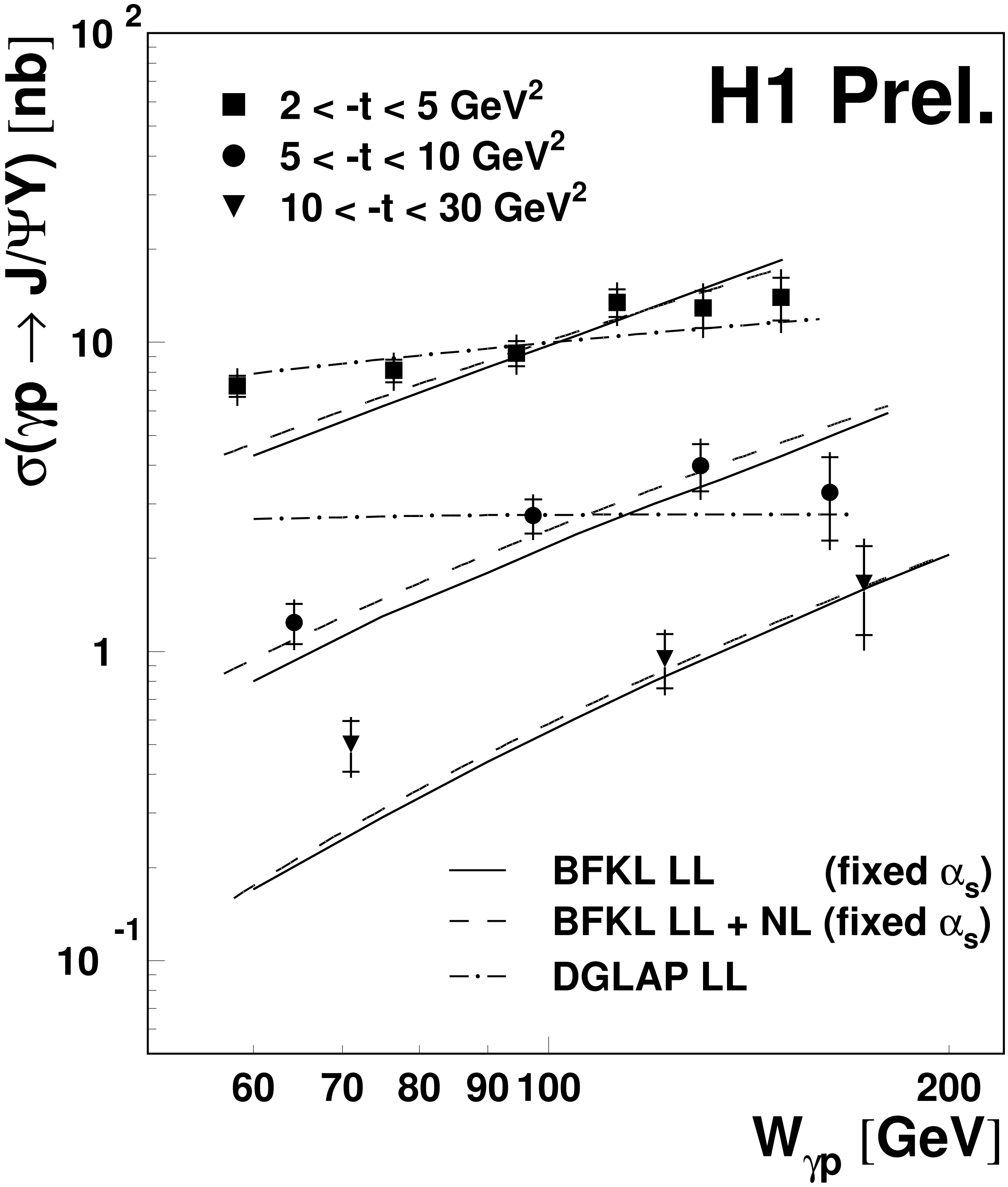

Figure 4: The photon-proton cross section as a function of $W_{\gamma p}$ in three bins of t. The inner error bars correspond to the statistical error, the outer error bars are the statistical and systematic errors added in quadrature. The solid lines show the predictions from the BFKL calculation in the leading log approximation and the dashed lines correspond to the results from the NL BFKL calculation using a fixed α_S [?]. Also shown (dashed-dotted curve) is the result of a calculation based on the DGLAP LL equation [?].

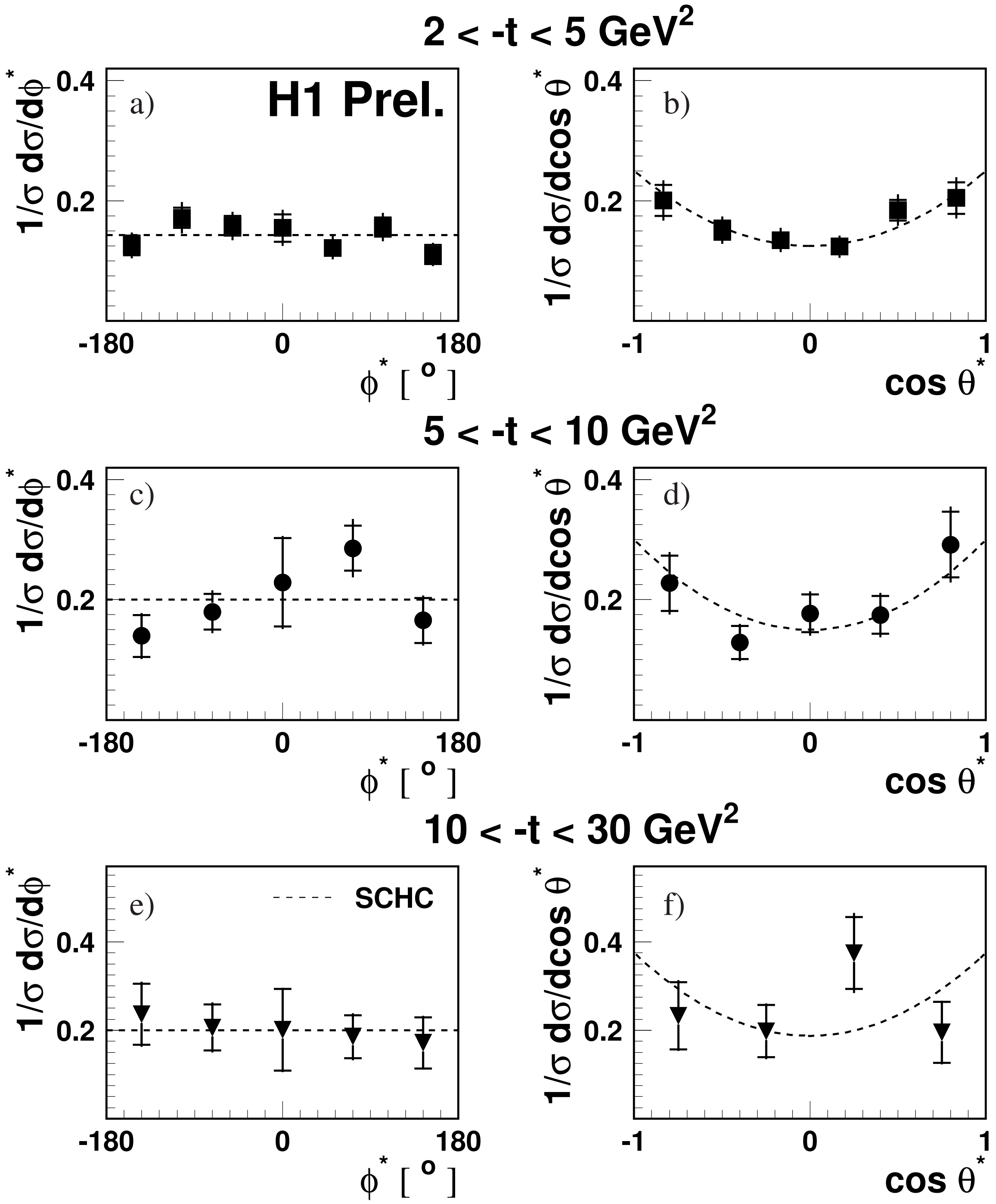

Figure 5: Normalised decay angular distributions for J/ψ meson production in three bins of t: a,b) $2 < |t| < 5$ GeV^2; c,d) $5 < |t| < 10$ GeV^2 and d,e) $10 < |t| < 30$ GeV^2. The left column(a,c,e) shows the azimuthal distributions ϕ^* of the positively charged decay muon in the helicity frame and the right column(b,d,f) shows the polar angular distributions $\cos\theta^*$. The inner error bars show the statistical error. The outer error bars include the statistical and systematical errors added in quadrature. The dashed line shows the expectation from s-channel helicity conservation.

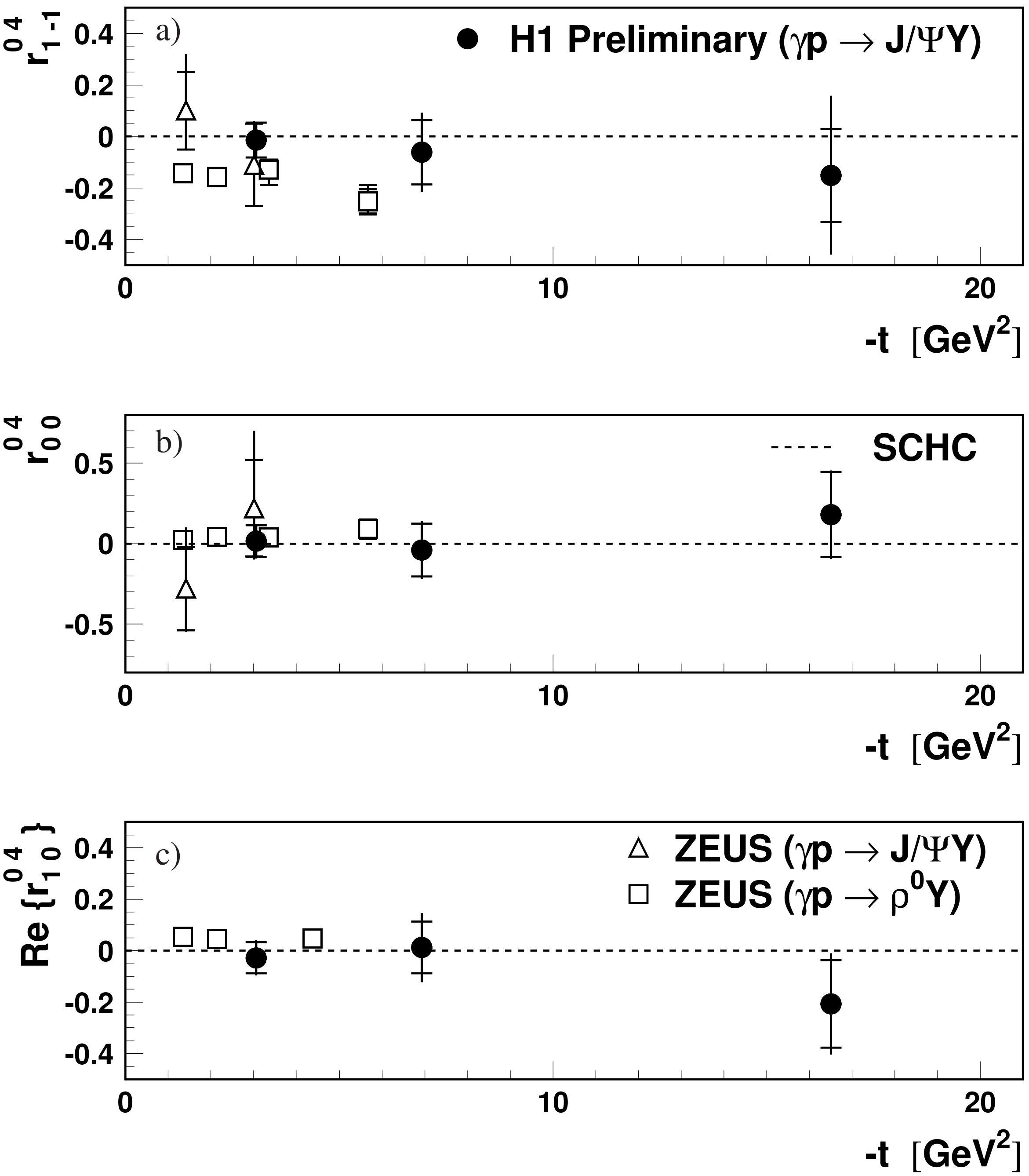

Figure 6: The three spin density matrix elements a) r^{04}_{1-1}, b) r^{04}_{00} and c) $\mathrm{Re}\{r^{04}_{10}\}$ for the J/ψ as a function of t. The inner error bars represent the statistical uncertainty and the outer error bars the combined statistical and systematic uncertainties. The dashed line shows the expectation from SCHC. Also shown on the figure are the results from the ZEUS collaboration for the photoproduction of J/ψ and ρ^0 mesons [?].